

A data-driven approach to η and η' Dalitz decays

Rafel Escribano^{1,2,*}

¹Grup de Física Teòrica, Departament de Física, Universitat Autònoma de Barcelona, E-08193 Bellaterra (Barcelona), Spain

²Institut de Física d'Altes Energies (IFAE), The Barcelona Institute of Science and Technology (BIST), Campus UAB, E-08193 Bellaterra (Barcelona), Spain

Abstract. Data-driven model-independent predictions for the dilepton invariant mass spectra and branching ratios of the single and double Dalitz decays $\eta^{(\prime)} \rightarrow \ell^+ \ell^- \gamma$ and $\eta^{(\prime)} \rightarrow \ell^+ \ell^- \ell^+ \ell^-$ ($\ell = e$ or μ) are provided by means of an approach based on the use of rational approximants applied to the available experimental data in the space-like region of the η and η' transition form factors.

1 Introduction

In this talk I have provided data-driven model-independent predictions for the dilepton invariant mass spectra and integrated branching ratios (BRs) of the single and double Dalitz decays $\eta^{(\prime)} \rightarrow \ell^+ \ell^- \gamma$ and $\eta^{(\prime)} \rightarrow \ell^+ \ell^- \ell^+ \ell^-$ with $\ell = e$ or μ . For a detailed and exhaustive analysis of all the processes considered, including the π^0 ones not reported here, I refer to the original work in Ref. [1]. It is worth noticing that the previous analysis is the first complete work including all the possible Dalitz reactions. Our approach is based on the use of rational approximants applied to the available experimental data in the space-like region of the η and η' transition form factors (TFFs) [2]. It is defined as model independent because we are able to ascribe a conservative systematic error to our predictions. In this sense, the traditional VMD description of the TFF in terms of a monopole used commonly by experimental collaborations must be considered only as a first step in this systematic approximation. For the case of the double Dalitz decays, which demand TFFs of double virtuality not yet experimentally available, we have made use of the factorization hypothesis stating that the normalised version of the double-virtual TFFs is nothing else than the product of the two single-virtual TFFs.

2 Transition form factors

The energy dependence of the η and η' TFFs in the time-like region required for describing these Dalitz decays has been predicted after fixing this dependence but from existing data in the space-like region reported by the CELLO [3], CLEO [4], L3 [5], and BABAR [6] collaborations. A more precise determination of these TFFs could have been obtained here taking into account in addition the recent data in the time-like region coming from the NA60 [7] ($\eta \rightarrow \mu^+ \mu^- \gamma$), A2 [8, 9] ($\eta \rightarrow e^+ e^- \gamma$) and BESIII [10] ($\eta' \rightarrow e^+ e^- \gamma$) Colls. Nevertheless, the impact of the incorporation of these

*e-mail: rescriba@ifae.es

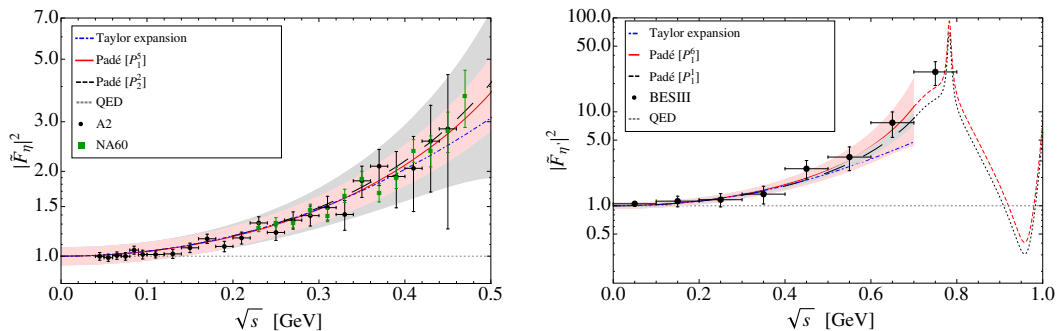


Figure 1. Modulus square of the normalised time-like η (left) and η' (right) TFF as a function of the invariant dilepton mass, $\sqrt{s} \equiv m_{\ell\ell}$. The predictions are compared to the experimental data from $\eta \rightarrow e^+e^-\gamma$ [9] (black circles), $\eta \rightarrow \mu^+\mu^-\gamma$ [7] (green squares) and $\eta' \rightarrow e^+e^-\gamma$ [10] (black circles).

sets of time-like data was studied in Refs. [11] and [12], for the η and η' cases, respectively. The application of Padé approximants (PAs) in the space-like is safe and reliable since the TFFs do not contain singularities in this region. The TFFs are expected to be well-behaved analytical functions except for a cut starting at the $\pi\pi$ threshold. The PAs, being rational functions and thus containing only poles by construction, are not sensitive to this unitary cut belonging to the time-like region. Therefore, one could think that PAs cannot be applied to this time-like region. However, it was shown in Ref. [12] that the effect of this unitary cut is minor and then one needs only to worry about the appearance of possible poles on the real (energy) axis that would prevent PAs from being used from that singularity on. Such poles could be understood as the projection on the real axis of resonance poles (or a combination of them) in the complex plane. For the η , the first pole encountered is well beyond the region of available phase-space and therefore its TFF is well established. For the η' , instead, the first pole appears in the upper part of the phase-space, somewhere inside the resonance region attributed to the lowest-lying vector mesons. For that reason, we match the η' TFF predicted by PAs to the more common VMD description to be able to predict the integrated BRs of the η' Dalitz decays (see Ref. [1] for details). In Fig. 1, our predictions for the the time-like region energy dependence of the η (left) and η' (right) TFFs are shown. We display the predictions for two different types of PAs, those with a single pole in the denominator, P_1^L , motivated by the likely dominance of resonances, and those diagonal, P_N^N , where the high-energy behaviour of the TFF predicted by perturbative QCD is imposed¹. The QED prediction (pointlike TFF) and the Taylor expansion including the slope and the curvature of the TFF are also included for comparison in each case. The error bands incorporate not only the statistical but also the systematic error associated to our approach. Higher the order of the PA is, smaller the systematic error is. In this line, the corresponding systematic uncertainty of a VMD description (monopole FF) is much bigger than ours. As seen, the agreement between our predictions for the two TFFs and the experimental data is remarkable, making the whole approach trustworthy.

3 Single Dalitz decays

For the numerical computations, we have employed the PDG fitted values $\Gamma_{\eta \rightarrow \gamma\gamma} = 0.516(18)$ keV and $\Gamma_{\eta' \rightarrow \gamma\gamma} = 4.35(14)$ keV [13]. In Fig. 2, we display the decay rate distributions for $\eta^{(\prime)} \rightarrow e^+e^-\gamma$

¹The fits in the space-like region were performed to $Q^2|F_{\eta^{(\prime)}}(Q^2)|$ and this behaves as a constant at high energies.

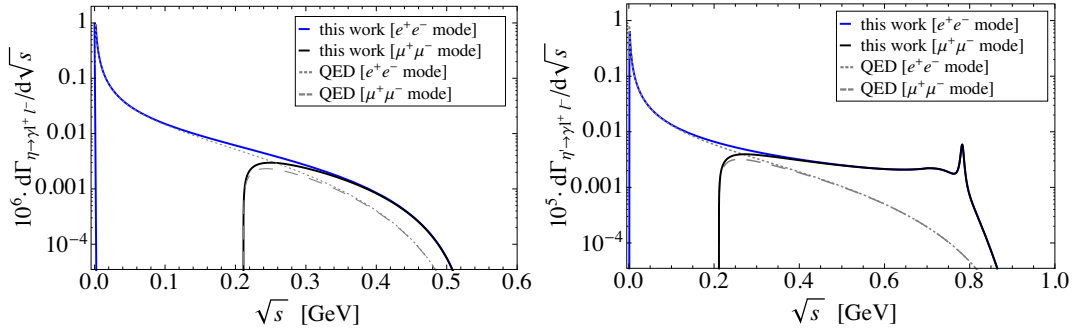


Figure 2. Decay rate distributions for $\eta^{(\prime)} \rightarrow e^+e^-\gamma$ (blue solid curves) and $\eta^{(\prime)} \rightarrow \mu^+\mu^-\gamma$ (black solid curves). The corresponding QED estimates are also displayed (grey dotted and long-dashed curves, respectively).

Table 1. Branching ratio predictions for $\eta \rightarrow \ell^+\ell^-\gamma$ ($\ell = e, \mu$) and their comparisons with experimental measurements and previous theoretical calculations.

Source	$\mathcal{BR}(\eta \rightarrow e^+e^-\gamma) \times 10^3$	$\mathcal{BR}(\eta \rightarrow \mu^+\mu^-\gamma) \times 10^4$
QED	6.38	2.17
This work (P_1^5)	$6.60^{+0.50}_{-0.47}$	$3.25^{+0.40}_{-0.36}$
This work (P_2^2)	$6.61^{+0.53}_{-0.49}$	$3.30^{+0.65}_{-0.56}$
PDG [13]	6.9 ± 0.4	3.1 ± 0.4
H. Berghauer <i>et al.</i> [8]	$6.6 \pm 0.4_{\text{stat}} \pm 0.4_{\text{syst}}$	
WASA-at-COSY Coll. [14]	$6.72 \pm 0.07_{\text{stat}} \pm 0.31_{\text{syst}}$	
QED [16]	6.38	2.18
FF 2,3 [17]	6.57	3.05
FF 4 [17]	6.53	2.87
LFQM [18]	6.95	2.94
Hidden gauge [19]	6.57 ± 0.03	3.05 ± 0.04
Modified VMD [19]	6.55 ± 0.03	2.97 ± 0.05

(blue solid curves) and $\eta^{(\prime)} \rightarrow \mu^+\mu^-\gamma$ (black solid curves). The non-pointlike behaviour of the TFFs is notably seen in the upper part of the spectra, being its numerical effect (in the integrated BRs) much bigger in the dimuon case than in the dielectron one for obvious phase-space reasons. Our BR predictions for $\eta^{(\prime)} \rightarrow \ell^+\ell^-\gamma$ ($\ell = e, \mu$) and their comparisons with experimental measurements and previous theoretical calculations can be found in Table 1, for the η , and Table 2, for the η' , respectively. As seen from the Tables, with the current precision, there is no difference within errors between the predictions from monopole PAs and diagonal ones. Indeed, at the level of integrated BRs, our predictions are incompatible with the QED ones only for the dimuon cases. In any case, the preferred channel for testing the energy dependence of the TFFs would be the radiative dimuon decay of the η' . At the present accuracy, however, there is not yet possible to distinguish among different theoretical frameworks. So far, all of them are compatible with each other and with the data. More refined experimental analyses will be required in the future.

Table 2. Branching ratio predictions for $\eta' \rightarrow \ell^+ \ell^- \gamma$ ($\ell = e, \mu$) and their comparisons with experimental measurements and previous theoretical calculations.

Source	$\mathcal{BR}(\eta' \rightarrow e^+ e^- \gamma) \times 10^4$	$\mathcal{BR}(\eta' \rightarrow \mu^+ \mu^- \gamma) \times 10^4$
QED	3.94	0.38
This work (P_1^6)	$4.42^{+0.39}_{-0.35}$	$0.81^{+0.16}_{-0.13}$
This work (P_1^1)	$4.35^{+0.29}_{-0.27}$	0.74 ± 0.06
PDG [13, 15]		1.08 ± 0.27
BESIII Coll. [10]	$4.69 \pm 0.20_{\text{stat}} \pm 0.23_{\text{sys}}$	
Hidden gauge [19]	4.62 ± 0.17	0.98 ± 0.05
Modified VMD [19]	4.53 ± 0.17	0.90 ± 0.05

Table 3. Central final branching ratio predictions as a combined weighted average of the results presented. Errors are symmetrised. n_σ stands for the number of standard deviations the measured results are from our predictions.

Decay	This work	Experimental value [13]	n_σ
$\pi^0 \rightarrow e^+ e^- \gamma$	1.169(1)%	1.174(35)%	0.15
$\eta \rightarrow e^+ e^- \gamma$	$6.61(50) \times 10^{-3}$	$6.90(40) \times 10^{-3}$	0.45
$\eta \rightarrow \mu^+ \mu^- \gamma$	$3.26(46) \times 10^{-4}$	$3.1(4) \times 10^{-4}$	0.26
$\eta' \rightarrow e^+ e^- \gamma$	$4.38(32) \times 10^{-4}$	$4.69(20)(23) \times 10^{-4}$	0.70
$\eta' \rightarrow \mu^+ \mu^- \gamma$	$0.75(6) \times 10^{-4}$	$1.08(27) \times 10^{-4}$	1.19
$\pi^0 \rightarrow e^+ e^- e^+ e^-$	$3.36689(5) \times 10^{-5}$	$3.34(16) \times 10^{-5}$	0.17
$\eta \rightarrow e^+ e^- e^+ e^-$	$2.71(2) \times 10^{-5}$	$2.4(2)(1) \times 10^{-5}$	1.38
$\eta \rightarrow \mu^+ \mu^- \mu^+ \mu^-$	$3.98(15) \times 10^{-9}$	$< 3.6 \times 10^{-4}$	
$\eta \rightarrow e^+ e^- \mu^+ \mu^-$	$2.39(7) \times 10^{-6}$	$< 1.6 \times 10^{-4}$	
$\eta' \rightarrow e^+ e^- e^+ e^-$	$2.10(45) \times 10^{-6}$	not seen	
$\eta' \rightarrow \mu^+ \mu^- \mu^+ \mu^-$	$1.69(36) \times 10^{-8}$	not seen	
$\eta' \rightarrow e^+ e^- \mu^+ \mu^-$	$6.39(91) \times 10^{-7}$	not seen	

4 Double Dalitz decays

For the double Dalitz decays, $\eta^{(\prime)} \rightarrow \ell^+ \ell^- \ell^+ \ell^-$ with $\ell = e$ or μ , we will mostly use the factorisation ansatz for the energy dependence of the doubly-virtual TFFs. However, bivariate approximants named Chisholm (CAs) can also be used. In these, besides the constraints imposed by perturbative QCD, one can implement OPE constraints as well. In both cases, the numerical predictions are indistinguishable. Again, the effect of the energy dependence of the TFFs is much bigger for the dimuon states, and in particular for the η' channels. Our predictions for the η and η' BRs involving two dielectron, two dimuon, and one dielectron and one dimuon final states are shown in the lower part of Table 3. Only the decay $\eta \rightarrow e^+ e^- e^+ e^-$ is measured at present. The other two η decays have upper bounds while nothing is known for the η' decays. There is some hope to measure in the near future the channels involving dielectron pairs but very unlikely for only dimuon pairs.

5 Conclusions

The detailed and exhaustive analysis performed in Ref. [1] can be summarised in Table 3, where central final branching ratio predictions as a combined weighted average of the results presented there are displayed, not only for those processes involving η and η' but also the π^0 ones for completeness.

This work was supported in part by the Ministerio de Economía y Competitividad under grants CICYT-FEDER-FPA 2014-55613-P and SEV-2012-0234, and the Secretaria d'Universitats i Recerca del Departament d'Economia i Coneixement de la Generalitat de Catalunya under grant 2014 SGR 1450.

References

- [1] R. Escribano and S. González-Solís, arXiv:1511.04916 [hep-ph]
- [2] R. Escribano, P. Masjuan and P. Sanchez-Puertas, Phys. Rev. D **89**, 034014 (2014)
- [3] H. J. Behrend *et al.* [CELLO Collaboration], Z. Phys. C **49**, 401 (1991)
- [4] J. Gronberg *et al.* [CLEO Collaboration], Phys. Rev. D **57**, 33 (1998)
- [5] M. Acciarri *et al.* [L3 Collaboration], Phys. Lett. B **418**, 399 (1998)
- [6] P. del Amo Sanchez *et al.* [BaBar Collaboration], Phys. Rev. D **84**, 052001 (2011)
- [7] R. Arnaldi *et al.* [NA60 Collaboration], Phys. Lett. B **677**, 260 (2009)
- [8] H. Berghauer *et al.*, Phys. Lett. B **701**, 562 (2011)
- [9] P. Aguár-Bartolome *et al.* [A2 Collaboration], Phys. Rev. C **89**, 044608 (2014)
- [10] M. Ablikim *et al.* [BESIII Collaboration], Phys. Rev. D **92**, 012001 (2015)
- [11] R. Escribano, P. Masjuan and P. Sanchez-Puertas, Eur. Phys. J. C **75**, 414 (2015)
- [12] R. Escribano, S. González-Solís, P. Masjuan and P. Sanchez-Puertas, Phys. Rev. D **94**, 054033 (2016)
- [13] K. A. Olive *et al.* [Particle Data Group Collaboration], Chin. Phys. C **38**, 090001 (2014)
- [14] P. Adlarson *et al.*, arXiv:1509.06588 [nucl-ex]
- [15] R. I. Dzhelyadin *et al.*, Sov. J. Nucl. Phys. **32**, 520 (1980) [Yad. Fiz. **32**, 1005 (1980)]
- [16] T. Miyazaki and E. Takasugi, Phys. Rev. D **8**, 2051 (1973)
- [17] F. Persson, hep-ph/0106130
- [18] C. C. Lih, J. Phys. G **38**, 065001 (2011)
- [19] T. Petri, arXiv:1010.2378 [nucl-th]